

Human Authentication By Matching 3d Skull With Face Image Using Scca

Dr.M.Pushparani

Professor & Head, Dept. of Computer science
Mother Teresa Women's University
drpushpa.mtwu@gmail.com

T.INDUMATHI ,PhD Scholar

Computer Science Department
Mother Teresa Women's University
Indumathi1979@yahoo.co.in

ABSTRACT:

In networked society the people perform many e-commerce activities in daily life. In such applications personal identification is critically important. Biometric identifiers are replacing traditional identifiers, as it is difficult to steal, replace, forget or transfer them. It is possible that, a 2D-image based facial recognition system can be easily spoofed with simple tricks and some poorly-designed systems have even been shown to be fooled by the imposters. Spoofing with photograph or video is one of the most common manners to circumvent a face recognition system. It becomes easier to spoof in these biometric systems with the aid of fake biometric; it further reduces the reliability and security of biometric system. In this paper, face spoof attack many biometric, applying skull identification. We will be exploring the techniques that are more secure and reliable. In skull identification, nearly all of the methods depend on accurate extraction and representation of the relationship between the skull and face. However, it is very difficult to extract this complex relationship. Because this work aims to identify human face is from skull. This paper proposes a skull identification method that matches a skull with enrolled faces, in which the mapping between the skull and face is obtained using enhance canonical correlation coefficient analysis with scale invariant feature transform (SIFT). Here a statistic method is adopted to estimate outlook from subclass of skull-face database using Principle component analysis and Linear discriminant analysis (LDA). In order to improve the accuracy of the result, we select the suitable organ (eyes, nose

and mouth) for the statistic result based on anatomy principle from the database and achieve the organ and face integration to build the final outlook, a method to build a joint statistical 3D model of the skull and face is presented. The Second approach for enhancing the matching performance of AAM is to AAM itself, by proposing a novel fitting algorithm or enhancing the existing fitting algorithms. In this proposed a fast AAM using enhance canonical correlation coefficient analysis (ECCCA), which has modeled the relation between differences of the image and the model parameter for improving the convergence speed of fitting algorithm. We propose to identify an skull through using a correlation measure between the 3D skull and 3D face in terms of the morphology, and measure the correlation using Enhance canonical correlation coefficient analysis (ECCCA) .We use the 3D skull data as the probe and 3D face geometric data as the gallery, and match the skull with enrolled 3D faces by the correlation measure between the probe and the gallery. The Third approach for scale invariant feature transform (SIFT) bundles a feature detector and a feature descriptor. The detector extracts from an image a number of frames (attributed regions) in a way which is consistent with (some) variations of the illumination, viewpoint and other viewing conditions.

Keywords: Security, Linear Discriminant Analysis(LDA), Principle Component Analysis (PCA), Active Appearance Modal (AAM), Enhance Canonical Correlation Coefficient Analysis (ECCCA), Scale Invariant Feature Transform (SIFT), Skull Identification

INTRODUCTION

Skull identification is one of the most important tasks in forensic anthropology. It has been practiced over one hundred years. Current research focuses mainly on craniofacial superimposition and craniofacial reconstruction. Both of them depend on accurate extraction and representation of the intrinsic relationship between the skull and face in terms of the morphology, which is difficult and still unsolved. Skull identification has been researched for over a century. Since the successful identification of relics of the famous German composer Bach in 1895, skull identification has drawn wide attention and been applied in huge number of forensic cases, ranging from the identification of victims of the Indian Ocean tsunami [2] to the identification of terrorists [3]. With the development of digitization technologies such as CT, 3D scanners etc., data acquisition becomes easier and easier, and human identification by skulls has been an interdisciplinary

research focus of informatics, anthropology, forensic sciences, and so on. Unlike other biological features such as DNA and fingerprinting, skull data for a living person still cannot be acquired in a convenient and non-intrusive way. Thus, skull identification cannot be realized in the same way as used by other biological feature identification technology, i.e., match-ing an unknown skull with a large skull database. Current skull identification research focuses mainly on two categories. One is craniofacial superimposition [6], [7], [14]–[18], and the other is craniofacial reconstruction [4], [5], [19]–[24].

Craniofacial superimposition firstly overlays the 2D projection of a 3D model of the unknown skull with a face photo of the missing person according to the same pose, and then, it makes an identification decision by assessment of the anatomical consistency of the cephalometric landmarks on the face photo and the skull projection. The superimposition is usually performed manually by forensic

anthropologists and requires special utilities and professional qualifications. Thus, the procedure of the identification is time-consuming and easily influenced by the subjectivity of the practitioners. Recently, a few automatic skull-face overlay methods have been proposed. These methods are based on evolutionary algorithms [14], [15], fuzzy logic [17], [18], and so on. For example, Ballerini et al [14] used a genetic algorithm to find the optimal transformation to match the landmarks on the 3D skull model and the face photo. Ibanez et al [18] used fuzzy logic to solve the uncertainty involved in the location of the cephalometric landmarks. Automatic methods need no tedious manual operation and can be easily reproduced. However, regardless of whether the method is automatic or non-automatic, it is difficult to fit a 2D image (the face photo) onto a 3D object (the skull). The reason is that the skull and face are two objects of different natures [16], which cause some inherent uncertainty in the matching. Moreover, accurate localization of craniofacial landmarks has been a longstanding problem in the field, and the uncertainty introduced by landmark localization also affects the matching.

Craniofacial reconstruction aims to estimate an individual's face appearance from its skull using the relationship between soft tissues and the underlying bone structure. It can provide a clue and trigger recognition by the victim's relatives, so that further identification evidence can be collected on a restricted list of candidates. Currently, craniofacial reconstruction is implemented manually by anatomists or artists. They physically model a face by adding clay or plasticize to a skull replica, relying on their experience. The reconstruction procedure is time consuming and prone to subjectivity. Most early computerized reconstruction methods [19], [20] obtained the face of the unknown target skull by deforming a craniofacial reference. They deform the reference skull to the target skull according to some skull features, and subsequently apply an extrapolation of the skull deformation to the reference face to obtain the reconstructed face. They assume that the reference and the unknown target individual have similar tissue thickness distributions. A model bias or unrealistic reconstructions always appear when an inappropriate reference is chosen [5]. Recent methods use statistical learning techniques, such as statistical shape models [21], [22], regression models [23], [24], etc., to explore the relationship between the skull and face, and the reconstruction is based on the learned relationship. However, the obtained statistical models depict only the craniofacial variation in a statistical sense and cannot reflect the personal variation. Thus, most reconstructed faces are not sufficiently accurate for identification.

In essence, both craniofacial superimposition and craniofacial reconstruction are based on a good grasp or representation of the relationship between the skull and face in terms of the morphology. However, how to accurately extract and represent the relationship is intractable and is still unsolved. They have a high uncertainty and a low identification capability. With the progress of 3D imaging technology, we expect that non-intrusive 3D face data

capture [8], [9] will become readily available and cost efficient. More importantly, 3D face modelling from images has received substantial attention [10]–[12]. So we believe that the acquisition of 3D face geometric models will become easier and easier.

In this earliest propose a novel technique for identifying an unknown skull based on the correlation measure between the 3D skull and 3D face in terms of the morphology. Using the 3D skull data as the probe and 3D face geometric data as the gallery, this approach matches the unknown skull with enrolled 3D faces by the correlation measure between the probe and the gallery. Unlike craniofacial superimposition and craniofacial reconstruction, this method does not require an accurate relationship between the skull and face. To boost the matching accuracy, we divide the skull and face skin into five physiological feature regions, establish five correlation analysis models, and make a decision by model fusion. Through this work, we prove that there is indeed a close relation between the skull and face, and thus, we provide a theoretical support for craniofacial superimposition and craniofacial reconstruction. On the other hand, we show that the region-based strategy is better than the holistic strategy in the extraction of the relationship between the skull and face, which provides an evidence for some research on regional craniofacial reconstruction.[35].

Face recognition also has disadvantages that come along with it. The face can be obstructed by hair, glasses, hats, scarves, etc. Also changes in lighting or facial expressions can throw off the device. A third disadvantage related to face recognition is that people's faces change over time. In order for face recognition to be accurate "images are most accurate when taken facing the acquisition camera and not sharp angles. Identity management using biometrics has nowadays become

a reality mainly because of the biometric passports (epassports) and also because of the presence of more and more biometric enabled-applications for personal computers. However, despite the significant progress in the recent decades

biometric systems are, unfortunately, vulnerable to attacks. A spoofing attack occurs when a person tries to masquerade as someone else by falsifying data and thereby gaining illegitimate access and advantages. This is currently a major problem for companies willing to market information security solutions based on biometric authentication technologies. The face spoofing in the world they can be applying for skull identification.

This paper proposes a skull identification method that matches skull with enrolled 3D faces, in which the mapping between the skull and face is obtained using enhance canonical correlation coefficient analysis with scale invariant feature transform. Unlike existing techniques, this method needs no accurate relationship between the skull and face, and measures only the correlation between them. In order to measure the correlation more reliably and improve the identification capability of the correlation analysis model, a region fusion strategy is adopted.

Firstly, a reliable skull identification technique is presented, and to the best of our knowledge, it is the first time that such a technique has been reported. Secondly, this paper proves that there is indeed a close relation between the skull and face in terms of the morphology, and thus, it proves the project for related research.

Thirdly, we show that the region-based strategy is better than of the extraction of the relationship between the skull and face; this finding supports further research on regional.

Firstly, we build a skull face database. Secondly, Here a statistic method is adopted to estimate outlook from subclass of skull-face database using Principle component analysis and Linear discriminant analysis LDA. In order to improve the accuracy of the result, we select the suitable organ (eyes, nose and mouth) for the statistic result based on anatomy principle from the database and achieve the organ and face integration to build the final outlook, a method to build a joint statistical 3D model of the skull and face is presented. This model is then used to reconstruct a face from available skull data. The idea is similar to, but uses a statistical shape model of both the skull and the face for the reconstruction task.

The Third approach for enhancing the matching performance of AAM is to modify the fitting algorithm of AAM itself, by proposing a novel fitting algorithm or enhancing the existing fitting algorithms. In this perspective [14] have proposed a fast AAM using the Enhance canonical correlation coefficient analysis (ECCCA), which has modeled the relation between differences of the image and the model parameter for improving the convergence speed of fitting algorithm. We propose to identify an skull through using a correlation measure between the 3D skull and 3D face in terms of the morphology, and measure the correlation using Enhance canonical correlation coefficient analysis (ECCCA) [13]. We use the 3D skull data as the probe and 3D face geometric data as the gallery, and match the skull with enrolled 3D faces by the correlation measure between the probe and the gallery.

The Fourth approach for scale invariant

Feature transform (SIFT) bundles a feature detector and a feature descriptor. The detector extracts from an image a number of frames (attributed regions) in a way which is consistent with (some) variations of the illumination, viewpoint and other viewing conditions. The descriptor associates to the regions a signature which identifies their appearance compactly and robustly.

Finally, the suitable organs (eyes, nose and mouth) are selected from organ database and we achieve the integration between organ and outlook to estimate final outlook of the skeleton remains. we show that the region-based strategy is better than the holistic strategy in terms of the extraction of the relationship between the skull and face.

II SKULL AND DATABASE

Each entry or item of skull-face database consists of two parts: skull model and face model. Here, we briefly describe the common method to achieve model digitalization and introduce the modal of our database. The study was carried by laboratory on a database of 150 hole head CT scans on

voluntary persons, More than 150 patients planned for preoperative surgery gave informed consent to scan the whole head for scientific research. The images of each subject are stored in DICOM 3.0 with 512×512 resolution. To get complete head data, 250 to 320 slices are captured for different persons. Most of the patients belong to the India. In this article, 110 samples are used for craniofacial reconstruction experiments. There are 48 female and 62 male subjects in the collection. The age distribution ranges from 20 to 60.

An entry (i.e. a sample) in our database consists of a skull surface coupled with a skin surface. For facial reconstruction, only the skull surface is known. These surfaces are represented by 3D meshes (vertices and triangles). In order to construct the statistical model, each skull or skin shape must share the same mesh connectivity. This particular connectivity arises from a subject-shared reference mesh (also denoted as generic mesh in the following). For each individual in our database, original meshes are reconstructed from CT data of the subject (Figure 1). The original CT slice images were processed by the model after filtering out the noise to extract the skull and face borders. The 3D skull and skin surfaces are reconstructed by a marching cubes algorithm [25], and they are represented as triangle meshes that include approximately 1 50,000 and 2 20,000 vertices, respectively. All of the heads are substantially complete. In detail, each skull contains all of the bones from calvarias to jaw and has a full mouth of teeth, and no face has a missing part. In addition, the subject's properties for each head, such as the age, gender, and body mass index (BMI), are stored. All of the information is self-reported by the participants. More of the details on the procedure for the data processing can be found in [26].

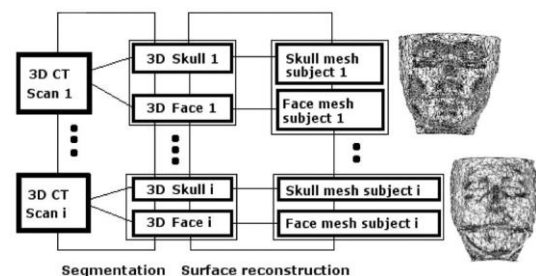


Fig.1 Mesh Reconstruct

To eliminate the inconsistency in the position, pose and scale caused by data acquirement, all of the samples are transformed into a uniform coordinate system. The uniform coordinate system is determined by four skull landmarks, the left porion, right porion, the left (or right) orbitale and the glabella (denote as L_p , R_p , L_o , G). From three points, L_p , R_p , L_o , the Frankfurt plane is determined [22]. The coordinate origin (denoted as O) is the intersection point of the line L_pR_p and the plane that contains point G and orthogonally intersects the line L_pR_p . We take the line OR_p as the x -axis. The z -axis is

the line through the point O, and it has the direction of the normal of the Frankfurt plane. Then, the y-axis is obtained by the cross product of the z- and x-axis. Once the uniform coordinate system is defined, all of the prototypic skins and skulls are transformed into it by a simple rotation and translation transformation. Finally, the scale of all of the samples is standardized by setting the distance between L_p and R_p to a unit, i.e., each vertex (x, y, z) of the skull and skin is scaled by $L^p - R^p$. The skull and face skin of one sample in the uniform coordinate system are shown in Figure.2. The original skull and skin meshes have different connectivity. In statistical learning, a dense point

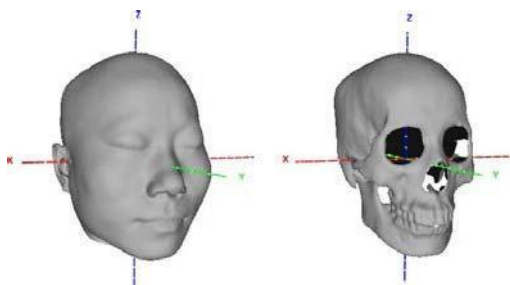


Fig. 2. One pair of skull and face in the uniform coordinates system.

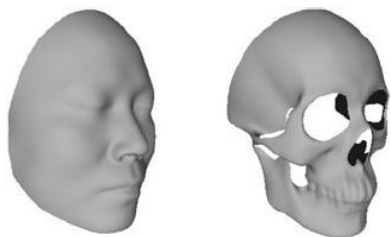


Fig. 3. The reference skull and face skin for data registration.

Correspondence must be established across the training set. As is known, the representation capability of statistical models depends critically on the quality of the correspondence. An inappropriate correspondence can cause the variation modes of the statistical model to not reflect the actual variation of the objects. Although there are many data registration methods for dense mesh or point cloud objects to establish the point correspondence, it is still a challenging problem to obtain accurate registration for dense skull and face meshes because there are complex non-rigid deformations among different craniofacial subjects. Here, we adopt the dense registration method described in [22]. It includes two steps. The first step is a non-rigid registration procedure using a fixed reference. The second step is to improve the registration by a linear combination model based on the first-step registered samples. This method reduces the model bias caused by a fixed reference at the cost of higher computational complexity. Fortunately, we do not need a real-time registration. Similar to the literature [22], we select one skull-and-face pair as a reference and cut away their back parts, considering that face recognition

mainly depends on the front part of the head. As shown in Figure 3, the reference skull and face have 41,059 and 40,969 vertices, respectively. After the data registration, all of the skulls and face skins have the same mesh connectivity as the reference one.

III METHODS

In skull identification, nearly all of the methods depend on accurate extraction and representation of the relationship between the skull and face. However, it is very difficult to extract this complex relationship. Because this work aims to identify an skull by looking for its corresponding face skin from a 3D face gallery, we measure only the correlation between a skull and a face skin, and do not need an accurate relationship.

A. Statistical Shape Model

Principal Component Analysis (PCA). In our experiments we implemented Principal Component Analysis (PCA) procedure as described by Turk and Pentland (1991). Given an s-dimensional vector representation of each face in a training set of M images, PCA tends to find a t-dimensional subspace whose basis vectors correspond to the maximum variance direction in the original image space. This new subspace is normally lower dimensional ($t \ll s$). New basis vectors define a subspace of face images called face space. All images of known faces are projected onto the face space to find sets of weights that describe the contribution of each vector. To identify an unknown image, that image is projected onto the face space as well to obtain its set of weights. By comparing a set of weights for the unknown face to sets of weights of known faces, the face can be identified. If the image elements are considered as random variables, the PCA basis vectors are defined as eigenvectors of the scatter matrix S_T defined as:

$$S_T = \sum_{i=1}^M (x_i - \mu) \cdot (x_i - \mu)^T \quad (1)$$

where μ is the mean of all images in the training set (the mean face, Fig. 4) and x_i is the i th image with its columns concatenated in a vector.

The projection matrix W_{PCA} is composed of t eigenvectors corresponding to t largest eigenvalues, thus creating a t-dimensional face space. Since these eigenvectors (PCA basis vectors) look like some ghostly faces they were conveniently named eigenfaces .

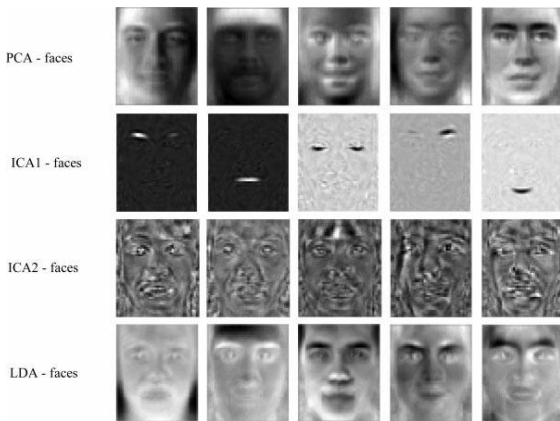


Fig.4 PCA and LDA Faces

B.Linear Discriminant Analysis (LDA). Linear Discriminant Analysis (LDA) (Belhumeur et al., 1996; Zhao et al., 1998) finds the vectors in the underlying space that best discriminate among classes. For all samples of all classes the between-class scatter matrix S_B and the within-class scatter matrix S_W are defined by:

$$S_B = \sum_{i=1}^c M_i \cdot (x_i - \mu) \cdot (x_i - \mu)^T \quad (2)$$

$$S_W = \sum_{i=1}^c \sum_{k \in X_i} (x_k - \mu_i) \cdot (x_k - \mu_i)^T \quad (3)$$

where M_i is the number of training samples in class i , c is the number of distinct classes, μ_i is the mean vector of samples belonging to class i and X_i represents the set of samples belonging to class i with x_k being the k -th image of that class. S_W represents the scatter of features around the mean of each face class and S_B represents the scatter of features around the overall mean for all face classes.

The goal is to maximize S_B while minimizing S_W , in other words, maximize the ratio $\det|S_B|/\det|S_W|$. This ratio is maximized when the column vectors of the projection matrix (W_{LDA}) are the eigenvectors of $S_W^{-1}S_B$. In order to prevent S_W to become singular, PCA is used as a preprocessing step and the final transformation is $W_{opt}^T = W_{LDA}^T W_{PCA}^T$

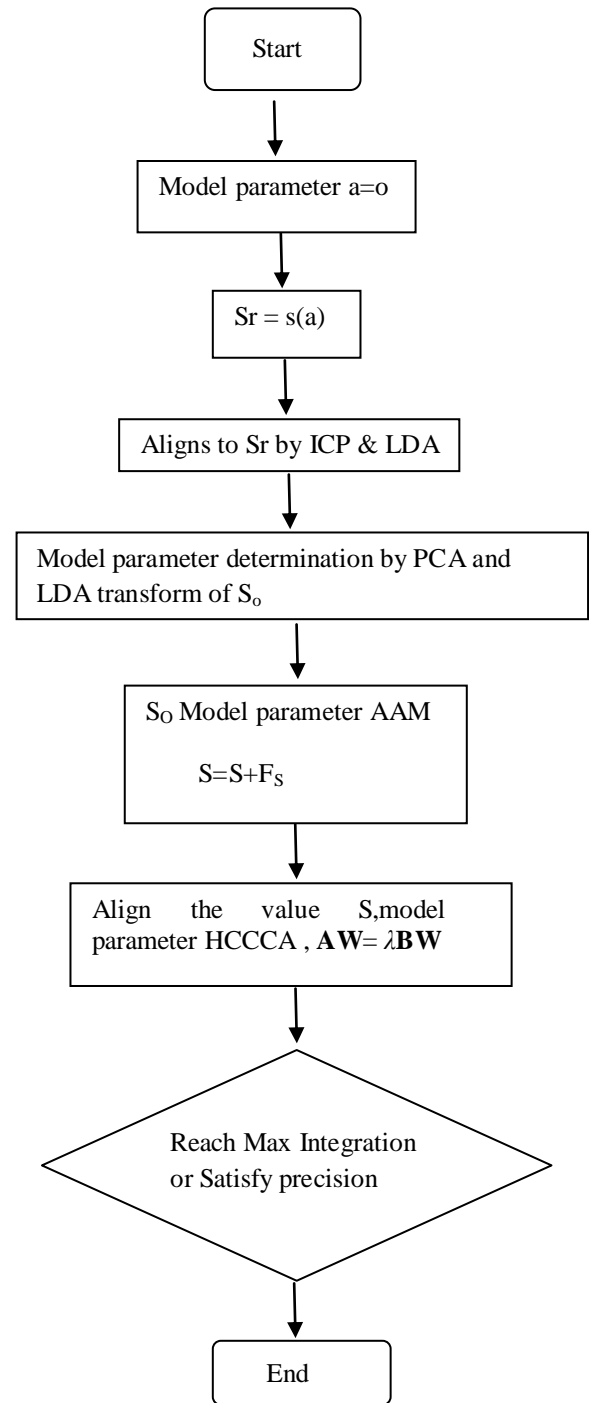


Fig.5 Model parameter procedure

C. Active Appearance Model:

Feature Extraction Using AAM Modeling. Given a set of training images, $I_i(x, y)$, $x = 0, 1, \dots, n-1$, $y = 0, 1, \dots, m-1$, and $i = 0, 1, \dots, N-1$, where $I_i(x, y)$ is of size $N \times M$. In the training images, the active portions have been manually labelled for extracting the parameters of the shape and appearance models.

In a 2D image landmark points can be represented as a 2n shape vector, X , where $X = (x_1, \dots, x_n, y_1, \dots, y_n)^T$. The set of shape vectors have been normalized to a common reference frame; hence X can be represented by x and by applying PCA:

$$S = S + Fs, \quad (4)$$

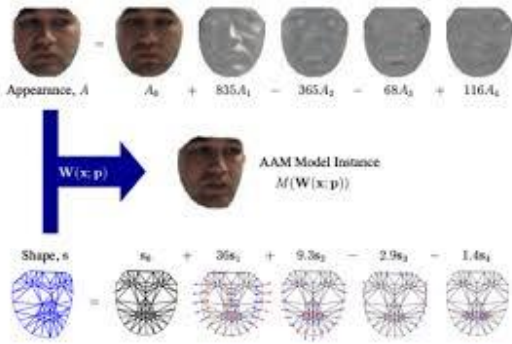


Fig.6 AAM modal

where S represents the synthesized shape in the normalized frame, S illustrates the mean shape in the normalized frame, F_s depicts the matrix of eigenvectors, extracted from the training shape, and ns is a set of shape parameters. In Fig6. after acquiring a shape model, every single training image has been distorted, where its control factors could match the mean shape. Next, the information is tested from the shape-normalized image, which is encompassed by the mean shape for forming a texture vector, G . A texture model might be constructed by applying PCA to the normalized texture vectors,

$$G = G + Fg, \quad (5)$$

where G is the synthesized texture in the normalized frame, G is the mean texture in the normalized frame, Fg is the matrix

which contains eigenvectors as columns, and ng is a set of texture parameters. The example of shape and texture can be synthesized by ns and ng . Since there are correlations between shape and texture variations, a weight matrix, should be

established for each shape parameter. Ws is a diagonal scaling matrix. Then a concatenated vector can be generated:

$$l = (ng \ Ws)^T = (Fg \ (G - G_0) \ Ws \ F_s^T \ (S - S_0)). \quad (6)$$

An appearance model will be set up by using a further PCA, $l = Qa$, $Q = (q_1 \ q_2 \ \dots \ q_n)$, (7)

where Q is the matrix which contains the eigenvectors as columns and a is a set of appearance parameter. Now a shape and texture model can be expressed by the appearance parameter, a ,

$$S = S + F_s \ W_s \ Q \ a, \quad G = G + F_g \ Q \ a. \quad (8)$$

D.CCA in the Shape Parameter Spaces

As described above, each training skull or face skin can be projected into its shape parameter space. That is, each skull has p feature variables, while each face skin has q

feature variables. Let $X_N \times p$ and $Y_N \times q$ denote the training skull and face data matrices, respectively, and let N denote the size of the training samples. The aim of HCCCA is to find two sets of basis vectors, $w_x \in \mathbb{R}^p$ and $w_y \in \mathbb{R}^q$, that maximize the correlation coefficient between the components $t_1 = Xw_x$ and $u_1 = Yw_y$, i.e.,

$$\rho = \max_{w_x, w_y} \frac{\text{cov}(t_1, u_1)}{\sqrt{\text{Var}(t_1) \times \text{Var}(u_1)}} \\ = \max_{w_x, w_y} \frac{w_x^T C_{xy} w_y}{\sqrt{w_x^T C_{xx} w_x \times w_y^T C_{yy} w_y}}$$

where the covariance matrices $C_{xy} = X^T Y$, $C_{xx} = X^T X$ and $C_{yy} = Y^T Y$.

Let $W = w_x^T$, w_y^T and $C_{yx} = Y^T X$, then Equation (4) can be solved by computing a generalized eigen-value decomposition problem, as follows:

$$AW = \lambda BW \quad (9)$$

where

$$A = \begin{pmatrix} 0 & C_{xy} \\ C_{yx} & 0 \end{pmatrix}, \quad B = \begin{pmatrix} C_{xx} & 0 \\ 0 & C_{yy} \end{pmatrix}. \quad (10)$$

More details on the derivation and solution of CCCA can be found in [13].

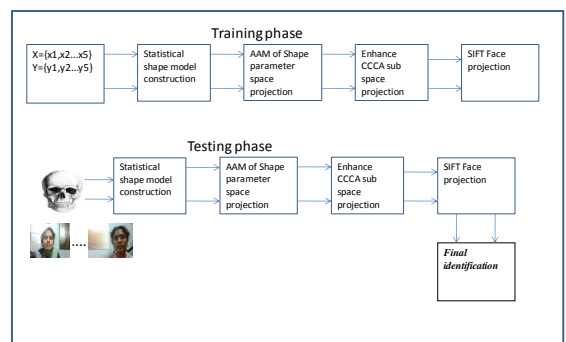


Fig. 7 SCCA based skull identification

Thus, we obtain two subspaces that consist of the basis vectors $w_x \in \mathbb{R}^p$ and $w_y \in \mathbb{R}^q$, respectively, for the skull and face skin. Assume that W_x denotes the subspace projection matrix whose columns are the basis vectors w_x , and W_y is the matrix that corresponds to the basis vectors w_y . For a skull-and-face pair, let x denote the shape parameter vector of the skull, and let y denote the shape parameter vector of the face. Then, the feature vectors of the skull and face in the

HCCCA subspaces are

$$\begin{aligned} \mathbf{x}_c &= \mathbf{W}_x^T \mathbf{x} \\ \mathbf{y}_c &= \mathbf{W}_y^T \mathbf{y}. \end{aligned} \quad (11)$$

We define the matching score between the skull and face as follows:

$$r(\mathbf{x}_c, \mathbf{y}_c) = \frac{\mathbf{x}_c \cdot \mathbf{y}_c}{\|\mathbf{x}_c\| \|\mathbf{y}_c\|} \quad (12)$$

where \cdot , $\|\cdot\|$ denotes the inner product operation.

E: Scale Invariant Feature Transform

In computer vision systems and pattern recognition, feature descriptors extracted from an image's gray values are usually used. Scale invariant feature transform (SIFT) is one of the best descriptors for feature matching. The SIFT algorithm transforms image data into scale-invariant coordinates relative to local features and is based on four major stages:

- Scale-space extrema detection: The image is first convolved with a series of Gaussian filters at different scales. Then, adjacent Gaussian images are subtracted to produce the difference-of-Gaussian images. Scale space extrema in the difference-of-Gaussians are regarded as the most stable scale-invariant features.
- Determination of keypoint location: Scale-space extrema are interpolated to obtain subpixel accuracy. Candidate keypoints with low contrast and those that are located along an edge but unstable to small amounts of noise are eliminated.
- Orientation assignment: This stage is the orientation assignment to each keypoint, based on local image gradient directions. This allows for the representation of each keypoint relative to this orientation, achieving invariance to image rotation. Peaks in orientation histogram are supposed to be dominant directions.
- Keypoint descriptor assignment: The previously described steps assigned the location, scale, and orientation of each keypoint. The motivation for the computation of a more complex descriptor is to obtain a highly distinctive keypoint and invariant as possible to variations. Each resultant SIFT descriptor is a 128-element feature vector.

After the keypoint descriptor has been calculated, keypoints are matched by using the minimum distance method, where an exhaustive search between all keypoints in both images is performed. In order to increase the stability of matching results, the ratio between the distance of the closest neighbor and the distance to the second closest neighbor is calculated to reject the matches. More details about SIFT. Despite the outstanding characteristics of the SIFT, it has some problems with image registration. Even after the identification of matching candidates after removal

of incorrect initial matches as described above, there are still many false matches due to feature points located in some similar structures, which lead to a further outlier removal.

IV IDENTIFICATION OF ORGANS

As organs (eyes, nose and mouth) are no relevant to the soft tissue thickness, suitable organs should be selected and merged with the estimated outlook to achieve craniofacial reconstruction.

Many researchers have done some research on the relations between organs and skull [12]. In this topic focuses on meshes registration and integration between organs and face. The processes of organ and face integration contain three steps: (1) Registering organ and face. (2) Deleting the organ of the estimated face. (3) Re-meshing to generate the final face. Initially at least three correspondence points of organ and the estimated face are picked up respectively.

Then SCCA is used to achieve rigid registration between

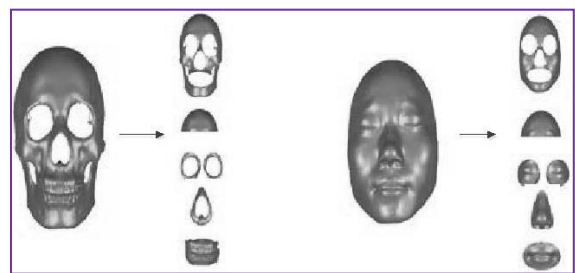


Fig.7 Skull and skin are decomposed into five regions according to physiological characteristics: profile, forehead, eyes, nose and mouth from up to down.

Region modes Table 1

Region	profile	Forehead	nose	Mouth
Identification rate	76%	81	35	20

organs and the estimated face. Finally, the organs of the original outlook are merged.

V. SKULL IDENTIFICATION

The aim of this work is to find the most probable face from a 3D face gallery for an skull. Thus, we must compute the matching score between the skull and each 3D face in the gallery and find the face with the highest matching score. The general framework for the skull identification is shown in Figure 6. Similar to typical machine learning-based applications, the procedure of the skull identification includes two phases, the training phase and the identification phase.

As Fig. 7 shows, in the training phase, the correlation analysis model is established. First, statistical shape models for skulls and faces are constructed using all of the training data, as Equations (1) and (2) describe; second, all of the training data are projected into the shape parameter spaces according to Equation (3); and third, HCCCA is performed for the shape parameter features of the training skulls and face skins, and two basis vectors, \mathbf{w}_x and \mathbf{w}_y , are obtained. In

the identification phase, the correlation analysis model is used to identify an unknown skull. First, the unknown skull and the face gallery are projected respectively into the shape parameter spaces by the statistical shape model matching described above; second, their shape parameter features are projected into the CCA subspaces according to Equation (11). Finally, the matching score between the unknown skull and each face in the gallery is computed according to Equation (12), and the face with the highest matching score is the identification result.

The identification result is surely not correct if the face gallery in a forensic case does not contain the face data of the unknown skull. Thus, it is important to evaluate the confidence of the identification result. Here, we use Bayes rule to compute the probability that the result is correct. For the identification result, we have two class labels, positive and negative. Let w_1 denote the positive status, and let w_2 denote the negative status.

According to Bayes rule, we compute the posterior probability that the matching score r belongs to the positive class, as follows:

$$P(w_1|r) = \frac{p(r|w_1)P(w_1)}{\sum_{j=1}^2 p(r|w_j)P(w_j)} \quad (13)$$

where $P(w_1)$ and $P(w_2)$ denote the prior probabilities, and $p(r|w_1)$ and $p(r|w_2)$ denote the class conditional probability density functions. If $P(w_1|r) > 0.5$, the matching is classified as a positive matching by the Bayes decision rule.

Let E denote the event that the face data of the unknown skull exists in the face gallery, and let $P(E)$ denote the probability of the event; then, we have

$$P(w_1) = P(w_1, E) = P(E)P(w_1|E) \\ P(w_2) = 1 - P(w_1) \quad (14)$$

where $P(w_1|E)$ denotes the correct identification probability with the condition that the face data of the unknown skull exists in the face gallery.

$P(E)$ is determined by prior information and the conditional probability density

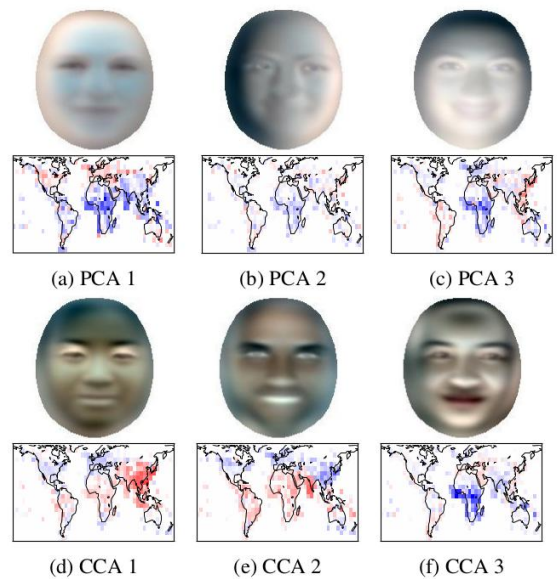


Fig. Different algorithm of image changes. functions $p(r|w_1)$ and $p(r|w_2)$ can be estimated by the matching score distribution of a data set. A detailed implementation is shown in the experiments and analysis section.

RESULT AND DISCUSSION

The used dataset is the 3D skull-and-face skin pairs of the 250 subjects described in Section II. Five-fold cross-validation was used to evaluate the proposed method. We randomly chose 7 non-overlapping data groups from the dataset, and each group included the 3D skull-and-face skin pairs of 30 subjects. For each fold, 30 skulls in one group were used as probes to test the proposed method, and the remaining 120 pairs of skull-and-face skins constitute the training set. In other words, we have 275 test skulls in all five folds. For each test skull, all of the 220 face skins constitute the gallery. The correct identification rate reported in the experiments is the average of the five folds. In this paper, we define that a test skull is identified at rank n , if the matching score of the correct match is of rank n . The identification rate at rank n is defined as the ratio of the cumulative count of the numbers of test skulls identified at rank n or less to the total number of test skulls. The correct identification rate is defined as the identification rate at rank 1. **EVALUATION OF SKULL IDENTIFICATION USING LDA AND PCA:**

Both Linear Discriminant Analysis (LDA) and Principal Component Analysis (PCA) are linear transformation techniques that are commonly used for dimensionality reduction. PCA can be described as an "unsupervised" algorithm, since it "ignores" class labels and its goal is to find the directions (the so-called principal components) that maximize the variance in a dataset. In contrast to PCA, LDA is "supervised" and computes the directions ("linear discriminants") that will represent the axes that maximize the separation between multiple classes. In Fig.8 compare the shape parameter.

Table 2 shape parameter LDA AND PCA

Region	Profile	forehead	Eye	nose	Mouth
Skull	74	67	30	33	65
Face	50	45	30	41	55

Although it might sound intuitive that LDA is superior to PCA for a multi-class classification task where the class labels are known, this might not always be the case.

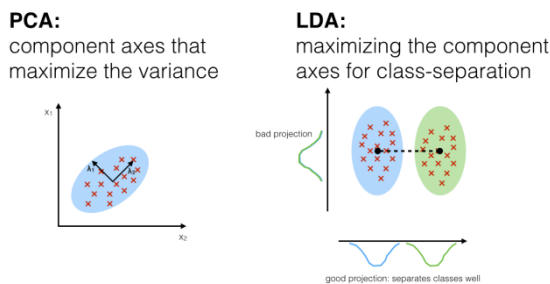


Fig. 8 Compare of PCA and LDA

Section III is discussed for shape parameter in skull and face. The PCA shape of face recognize the database, to identify unknown image, that image is projected onto the face space as well to obtain its set of weights. By comparing a set of weights for the unknown face to sets of weights of known faces, the face can be identified. If LDA shape and near the PCA and maximizing the component axes for face space.

II.Evaluation of skull identification using Enhance canonical correlation coefficient analysis.

For each fold, we built an enhance correlation analysis model in which all of the 176 eigen-vectors are used to construct the statistical shape models. A total of 150 test skulls were correctly identified at rank 1. The correct identification rate attained 81.5%. It verifies that there indeed exists some relationship between the skull and face, and it also shows that the proposed skull identification method is effective.

To describe the confidence evaluation of the identification result presented in Section III, four test groups in four folds are used to estimate the probability distributions of the positive matching (i.e., the matching between a skull with its corresponding face) and the negative matching (i.e., the matching between a skull with the faces of other persons), and the identification results of the 40 test skulls in the remaining one fold are used for the confidence evaluation. In this part, the former four test groups are referred to as the probability training set, while the latter 40 test skulls are referred to as the evaluation set. We perform statistical analysis for the 25600 ($4 \times 40 \times 160$) matching scores that were derived from the probability training set. The mean and standard deviation are (0.3205, 0.0811) for the positive matching and (0.0009, 0.0806) for the negative matching. Figure 6a and 6b show the histograms of the matching scores for the positive and negative matching, respectively. From Figure 6, we can see that both the positive and negative matching score approximately follow a Gaussian distribution. Thus, the two class conditional probability

density functions can be set as Gaussian distributions, with the mean and standard deviation computed for the positive and negative matching, respectively. Figure 9c shows the two standard Gaussian distributions. We can see that the scores of the positive and negative matching are separable. The conditional probability $P(w_1|E)$ in Equation (14) can be set as the average correct identification rate of the four folds that the probability training set belongs to, i.e., 80.6%. The prior probability $P(E)$ can be set to 1 because all of the face data of the test skulls exists in the face gallery in this experiment. According to the Bayes decision rule, we evaluate the identification results of the evaluation set, i.e., the 40 test skulls in the remaining one fold. Five of the 6 false identification results and all of the 34 correct results are classified as positive. If we set $P(E)$ as 0.5, i.e., we have no prior information about whether the face data of the test skull exists in the face gallery, then one correct identification result is classified as negative and 3 false results are classified as positive. By performing analysis of there are two cases for the false identification skulls. One case is that both the correct matching score and the mismatched score are low, and this case can be classified as negative matching. The

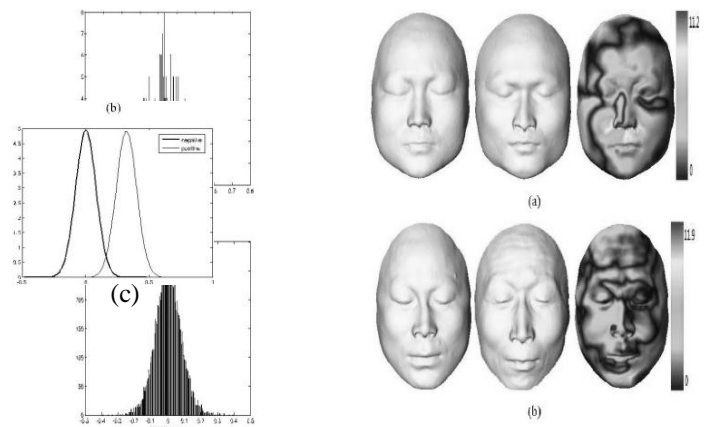


Fig. 9. Histograms of matching scores for the positive matching (a), negative matching (b), and class conditional probability density functions (c).

Table3 correlation coefficient analysis

region	Profile	Forehead	Eye	nose	mouth
Skull	85	77	65	75	85
Face	75	75	80	81	85

Other case is that the global morpho-logical similarity between the mismatched face and the true face is high, and it can be misclassified as positive matching. Figure 9 shows two samples of the second case. We can see that the mismatched faces are visually similar to the true faces. Figure 9 also shows the comparison colored from blue to red according to the geometric distance between the two faces. The average distances of these two samples are 2.7 mm and 2.56 mm, respectively. From the colored comparisons, we can see that the distance between the mismatched faces and the true faces is very small in most of the regions. The

global morphological similarity between two faces leads to similar shape model parameters, which contribute to the false matching due to a holistic model. For this reason, we propose the region-based method.

CONCLUSION:

In skull identification, nearly all of the methods depend on accurate extraction and representation of the relationship between the skull and face. However, it is very difficult to extract this complex relationship. Because this work aims to identify human face is from skull. This paper proposes a skull identification method that matches a skull with enrolled faces, in which the mapping between the skull and face is obtained using enhance canonical correlation coefficient analysis with scale invariant feature transform (SIFT).

The first build this statistical model, a 3D-to-3D matching procedure delivers subject specific meshes of the skull and face with the same number of vertices. A shared normalized space for the faces and skulls is therefore built. The direct statistical relationships between the face and the skull included in the statistical model are used to reconstruct the data from the face when the skull is the only available information.

Second of them depend on accurate extraction and representation of the intrinsic relationship between the skull and face in terms of the morphology, which is difficult and still unsolved. In these technique for identifying an skull based on the correlation measure between the 3D skull and 3D face in terms of the morphology. Using the 3D skull data as the probe and 3D face geometric data as the gallery, this approach matches the skull with enrolled 3D faces by the correlation measure between the probe and the gallery.

Third approach is a mismatching elimination algorithm, inspired by SCCA, has been proposed to improve the accuracy

of the SIFT-based method for the image registration problem. This algorithm is applicable to various images with different images, acquisition times, and scene changes. The core of the proposed method was to impose spatial relationship of matching features by means of SCCA to reject outliers. The experimental results on a variety of multisource remote sensing image pairs proved the method's advantages in terms of robustness and accuracy. Despite the effectiveness of the proposed approach, many developments need to be considered in the future work, including the choice of threshold and the algorithm efficiency.

In this work, we only use CT scan data to validate the proposed method. 3D face data acquisition by CT is infeasible for real applications because of the intrinsic radiation for the livings and the cost of the system. Compared with CT scan, 3D face modelling from 2D images is a convenient and non-intrusive way. By this way, we can construct a 3D face database from a 2D database of persons in a nation. Therefore, future work will focus on how to live face change to live skull modal to our database applying the proposed technique to 3D face models reconstructed the field of public security.

Acknowledgment

CT scans data have been collected for several subjects thanks to the laboratory and voluntary person.

REFERENCES

- D. Dirkmaat, *A Companion to Forensic Anthropology*. Hoboken, NJ, USA: Wiley, 2012.
- S. Al-Amad, M. McCullough, J. Graham, J. Clement, and A. Hill, "Craniofacial identification by computer-mediated superimposition," *Forensic Odontostomatol.*, vol. 24, no. 2, pp. 47–52, 2006.
- E. Indriati, "Historical perspectives on forensic anthropology in Indonesia," in *Handbook of Forensic Anthropology and Archaeology*,
- Blau and D. H. Ubelaker, Eds. Walnut Creek, CA, USA: Left Coast Press, 2009, pp. 115–125.
- C. Wilkinson, *Forensic Facial Reconstruction*. Cambridge, U.K.: Cambridge Univ. Press, 2004.
- P. Claes, D. Vandermeulen, S. De Greef, G. Willems, J. G. Clement, and P. Suetens, "Computerized craniofacial reconstruction: Conceptual framework and review," *Forensic Sci. Int.*, vol. 201, nos. 1–3, pp. 138–145, 2010.
- S. Damas *et al.*, "Forensic identification by computer-aided craniofacial superimposition: A survey," *ACM Comput. Surv.*, vol. 43, no. 4, pp. 1–27, 2011.
- W. A. Aulsebrook, M. Y. I. scan, J. H. Slabbert, and P. Becker, "Superimposition and reconstruction in forensic facial identification: A survey," *Forensic Sci. Int.*, vol. 75, nos. 2–3, pp. 101–120, 1995.
- [8] T. Beeler, B. Bicke, P. Beardsley, B. Sumner, and M. Gross, "High-quality single-shot capture of facial geometry," *ACM Trans. Graph.*, vol. 29, no. 4, pp. 40-1–40-9, 2010.
- [9] D. Bradley, W. Heidrich, T. Popa, and A. Sheffer, "High resolution passive facial performance capture," *ACM Trans. Graph.*, vol. 29, no. 4, pp. 41-1–41-10, 2010.
- [10] C. J. Kuo, R.-S. Huang, and T.-G. Lin, "3-D facial model estimation from single front-view facial image," *IEEE Trans. Circuits Syst. Video Technol.*, vol. 12, no. 3, pp. 183–192, Mar. 2002.
- [11] S.-Y. Baek, B.-Y. Kim, and K. Lee, "3D face model reconstruction from single 2D frontal image," in *Proc. 8th Int. Conf. Virtual Reality Continuum Appl. Ind.*, Yokohama, Japan, Dec. 2009, pp. 95–101.
- [12] M. Dimitrijevic, S. Ilic, and P. Fua, "Accurate face models from uncalibrated and ill-lit video sequences," in *Proc. IEEE Comput. Soc. Conf. Comput. Vis. Pattern Recognit. (CVPR)*, Jun./Jul. 2004, pp. 1034–1041.
- [13] D. R. Hardoon, S. Szedmak, and J. Shawe-Taylor "Canonical correlation analysis: An

- overview with application to learning methods,” *Neural Comput.*, vol. 16, no. 12, pp. 2639–2664, 2004.
- [14] L. Ballerini, O. Cordón, J. Santamaria, S. Damas, I. Aleman, and M. Botella, “Craniofacial superimposition in forensic identification using genetic algorithms,” in *Proc. 3rd Int. Symp. Inf. Assurance Security*, 2007, pp. 429–434.
 - [15] O. Ibáñez, L. Ballerini, O. Cordón, S. Damas, and J. Santamaria, “An experimental study on the applicability of evolutionary algorithms to craniofacial superimposition in forensic identification,” *Inf. Sci.*, vol. 179, no. 23, pp. 3998–4028, 2009.
 - [16] T. W. Fenton, A. N. Heard, and N. J. Sauer, “Skull-photo superimposition and border deaths: Identification through exclusion and the failure to exclude,” *J. Forensic Sci.*, vol. 53, no. 1, pp. 34–40, 2008.
 - [17] J. Santamaria, O. Cordón, S. Damas, and O. Ibaez, “Tackling the coplanarity problem in 3D camera calibration by means of fuzzy land-marks: A performance study in forensic craniofacial superimposition,” in *Proc. IEEE 12th Int. Conf. Comput. Vis. Workshop (ICCV)*, Oct. 2009, pp. 1686–1693.
 - [18] O. Ibáñez, O. Cordón, S. Damas, and J. Santamaria, “Modeling the skull–face overlay uncertainty using fuzzy sets,” *IEEE Trans. Fuzzy Syst.*, vol. 19, no. 5, pp. 946–959, Oct. 2011.
 - [19] D. Vandermeulen, P. Claes, D. Loeckx, S. De Greef, G. Willems, and P. Suetens, “Computerized craniofacial reconstruction using CT-derived implicit surface representations,” *Forensic Sci. Int.*, vol. 159, pp. S164–S174, May 2006.
 - [20] S. Michael and M. Chen, “The 3D reconstruction of facial features using volume distortion,” in *Proc. 14th Eurograph. U.K. Conf.*, 1996, pp. 297–305.
 - [21] P. Claes, D. Vandermeulen, S. De Greef, G. Will
ems, J. G. Clement, and P. Suetens, “Bayesian estimation of optimal craniofacial reconstructions,” *Forensic Sci. Int.*, vol. 201, nos. 1–3, pp. 146–152, 2010.
 - Y. Hu *et al.*, “A hierarchical dense deformable model for 3D face reconstruction from skull,” *Multimedia Tools Appl.*, vol. 64, no. 2, pp. 345–364, 2013.
 - M. Berar, F. M. Tilotta, J. A. Glaunès, and Y. Rozenholc, “Craniofacial reconstruction as a prediction problem using a latent root regression model,” *Forensic Sci. Int.*, vol. 210, nos. 1–3, pp. 228–236, 2011.
 - F. Duan, S. Yang, D. Huang, Y. Hu, Z. Wu, and M. Zhou, “Craniofacial reconstruction based on multi-linear subspace analysis,” *Multimedia Tools Appl.*, Jan. 2013, doi: 10.1007/s11042-012-1351-2.
 - W. E. Lorensen and H. E. Cline, “Marching cubes: A high resolution 3D surface construction algorithm,” *ACM SIGGRAPH Comput. Graph.*, vol. 21, no. 4, pp. 163–169, 1987.
 - Q. Deng, M. Zhou, W. Shui, Z. Wu, Y. Ji, and R. Bai, “A novel skull registration based on global and local deformations for craniofacial reconstruction,” *Forensic Sci. Int.*, vol. 208, nos. 1–3, pp. 95–102, 2011.
 - W. Yang, D. Yi, Z. Lei, J. Sang, and S. Z. Li, “2D–3D face matching using CCA,” in *Proc. 8th IEEE Int. Conf. Autom. Face Gesture Recognit. (FG)*, Sep. 2008, pp. 1–6.
 - B. Abraham and G. Merola, “Dimensionality reduction approach to multivariate prediction,” *Comput. Statist. Data Anal.*, vol. 48, no. 1, pp. 5–16, 2005.
 - W. Zheng, X. Zhou, C. Zou, and L. Zhao, “Facial expression recognition using kernel canonical correlation analysis (KCCA),” *IEEE Trans. Neural Netw.*, vol. 17, no. 1, pp. 233–238, Jan. 2006.
 - P. J. Besl and N. D. McKay, “A method for registration of 3-D shapes,” *IEEE Trans. Pattern Anal. Mach. Intell.*, vol. 14, no. 2, pp. 239–256, Feb. 1992.
 - P. Tu, R. Book, X. Liu, N. Krahnstoever, C. Adrian, and P. Williams, “Automatic face recognition from skeletal remains,” in *Proc. IEEE Conf. Comput. Vis. Pattern Recognit. (CVPR)*, Jun. 2007, pp. 1–7.
 - J. Huang, M. Zhou, F. Duan, Q. Deng, Z. Wu, and Y. Tian, “The weighted landmark-based algorithm for skull identification,” in *Proc. 14th Int. Conf. Comput. Anal. Images Patterns (CAIP)*, LNCS 6855, 2011, pp. 42–48.
 - Y. Hu, F. Duan, M. Zhou, Y. Sun, and B. Yin, “Craniofacial reconstruction based on a hierarchical dense deformable model,” *EURASIP J. Adv. Signal Process.*, vol. 2012, p. 217, Oct. 2012.
 - G. M. Gordon and M. Steyn, “An investigation into the accuracy and reliability of skull-photo superimposition in a South African sample,” *Forensic Sci. Int.*, vol. 216, nos. 1–3, pp. 198.e1–198.e6, 2012.
 - Fuqing Duan, Yanchao Yang, Yan Li, Yun Tian, Ke Lu, Zhongke Wu, and Mingquan Zhou” Skull Identification via Correlation Measure Between Skull and Face Shape” *IEEE transactions on information forensics and Security*, vol. 9, no. 8, august 2014